



Analytical Solutions for Water Infiltration into Unsaturated–Semi-Saturated Soils Under Different Water Content Distributions on the Top Boundary

Hamed Reza Zarif Sanayei¹ · Nasser Talebbeydokhti^{2,3} · G. Reza Rakhshandehroo²

Received: 31 May 2018 / Accepted: 28 January 2019 / Published online: 9 February 2019
© Shiraz University 2019

Abstract

Modeling and simulation of water infiltration from the ground surface into unsaturated–saturated soil is very important in the study of the hydrological cycle process. Transient fluid flow through unsaturated–saturated soil is generally described by Richards' equation. The equation is a nonlinear parabolic partial differential equation for which many numerical and limited analytical solutions exist. In this paper, exponential models for water content and hydraulic conductivity are selected so the nonlinear equation becomes linear and then separation of variables and Fourier series expansion techniques are used to derive analytical solutions to 2D water infiltration into unsaturated–semi-saturated soils with different distributions of water content on a part and/or parts of the top boundary. 2D water infiltrations are investigated in a rectangular soil domain, where high water content zone is considered as semi-saturated zone and residual water content zone is considered as unsaturated zone at initial time. A total of three cases are investigated in this paper. In case 1, a uniform distribution of water content on a part at the top boundary and no-flow boundaries at side edges are considered. Also, horizontal water table in unsaturated–semi-saturated domain is assumed as initial condition. In case 2, an inclined water table initial condition and a uniform distribution of water content on a part at the top boundary are investigated. Finally, in case 3, an analytical solution for ramp distributions of water content on two parts at the top boundary and an inclined water table initial condition is obtained. To illustrate the use of the derived equations, water content values are obtained from a numerical solution and compared to those from analytical solutions for two cases, showing less than 2% errors. These analytical solutions may be used as a benchmark for verification and efficiency assessment of numerical approaches.

Keywords Analytical solution · Water infiltration · Unsaturated–semi-saturated soil · Two dimension · Richards' equation · Inclined water table

1 Introduction

Simulation and estimation of water infiltration from the ground surface into unsaturated–saturated soil is an important discussion for the study of the hydrological cycle process. Also, recharge and discharge of the groundwater should

be carried out from the unsaturated to saturated zone and/or inverse, and therefore, the investigation of the transport process of water flow in soil is essential for the water resources management.

Transient fluid flow through unsaturated–saturated soil is generally described by Richards' equation derived by combining Darcy's law and conservation of mass. The equation is a nonlinear parabolic partial differential equation (PDE) for which many numerical and limited analytical solutions exist.

However, the choice of exponential model for water content and hydraulic conductivity linearizes the nonlinear Richards' equation, making it possible to obtain an analytical solution via classical approaches.

In the literature, many numerical methods have been suggested to investigate water flow infiltration through

✉ Hamed Reza Zarif Sanayei
hzarif63@gmail.com; zarif@sku.ac.ir

¹ Faculty of Engineering, Shahrood University, Shahrood, Iran

² Department of Civil and Environmental Engineering, Shiraz University, Shiraz, Iran

³ Environmental Research and Sustainable Development Center, Shiraz University, Shiraz, Iran

unsaturated–saturated soils. These techniques include finite difference method (FDM), finite element method (FEM), finite volume method (FVM) and/or other numerical methods (Zhu et al. 2011, 2012; Mousavi Nezhad et al. 2011; Carr and Turner 2014; Aquino et al. 2007; Simunek 2006; Zambra et al. 2012).

Analytical solutions, on the other hand, are mainly offered for one-dimensional flow of water through the soil and for restrictive boundary and initial conditions. Exact analytical solutions are desirable because they give a better insight compared with a discrete numerical solution.

Chen and Tan (2005) simulated the progress of the soil water content distribution in the soil profile with a water table at the bottom of the soil profile during ponding irrigation. This simulation was presented by solving the two-dimensional Richards' equation which used exponential functions for the hydraulic conductivity and volumetric water content. Craig et al. (2010) presented a new set of formulae for calculating regionally averaged infiltration rates into heterogeneous soils. The solutions were based upon an upscaled approximation of the explicit Green–Ampt (GA) infiltration solution and required specification of the spatial distribution of saturated hydraulic conductivity and/or initial soil water deficit in the sub-basin. Tong et al. (2010) developed a one-dimensional, two-layer solute transport model to simulate chemical transport process in an initially unsaturated soil with ponding water on the soil surface before surface runoff starts. The developed mathematical model was tested against a laboratory experiment. Zhan et al. (2013) developed an analytical solution for simulating rainfall infiltration into an infinite unsaturated soil slope. The analytical solution was based on the general partial differential equation for water flow through unsaturated soils. Numerical simulations were conducted to verify the assumptions of the analytical solution and demonstrated that the proposed analytical solution was acceptable for the coarse soils with low air entry values. Zarif Sanayei et al. (2016) derived new analytical solutions to 2D vertical and horizontal infiltration and imbibition into unsaturated soils for non-symmetrical boundary and non-uniform initial conditions. In that paper, presented analytical solutions were such that both steady and unsteady solutions could be obtained from a single closed-form solution. Also, comparing analytical solutions with numerical solutions showed a maximum error of less than 2%.

Cui and Zhu (2018) developed a new analytical infiltration model to determine water flow dynamics around layer interfaces during infiltration process in layered soils. The model mainly involved the analytical solutions to quadratic equations to determine the flux rates around the interfaces. Also, comparison to the numerical solutions of the Richards equation indicated that the new model can well capture water dynamics in relation to the arrangement of soil layers. Li and

Wei (2018) presented an approximate analytical solution for the coupled seepage and deformation problem of unsaturated soils. In that paper, these coupled governing equations were linearized and analytically solved for a specified saturation using the eigenfunction method. Also, comparison between the analytical solution and the previous theoretical solution indicated that the proposed solution yields excellent results.

A number of researchers investigated analytical solutions to the Richards' equation by variational iteration method (VIM), Adomian decomposition method (ADM), traveling wave solution (TWS), separation of variables and other analytical methods (Wazwaz 2007; Nasseri et al. 2008; Zlotnik et al. 2007; Zarif Sanayei et al. 2017; Johari and Hooshmand 2015; Wang et al. 2017; Su et al. 2017).

In this study, separation of variables and Fourier series expansion techniques are used to derive analytical solutions to 2D water infiltration into unsaturated–semi-saturated soils with different distributions of water content on a part and/or parts of the top boundary. 2D water infiltrations are investigated for a rectangular soil domain, where high water content zone is considered as semi-saturated zone and residual water content zone is considered as unsaturated zone at initial time. A total of three cases are investigated in this paper. In case 1, a uniform distribution of water content on a part at the top boundary and no-flow boundaries at side edges are considered. Also, horizontal water table in unsaturated–semi-saturated domain is assumed as initial condition. In case 2, an inclined water table initial condition and a uniform distribution of water content on a part at the top boundary are investigated. Finally, in case 3, an analytical solution for ramp distributions of water content on two parts at the top boundary and an inclined water table initial condition is obtained. Analytically, setting up and developing of these boundary and initial conditions for the cases are the main innovations of this research.

To illustrate the use of the derived equations, water content values from a numerical solution are compared to that from an analytical solution for two cases. These analytical solutions may be used as a benchmark for verification and efficiency assessment of numerical approaches. Also, these can be applied as the benchmark solutions which are vital for several analyses such as sensitivity analysis.

2 Governing Equation for Water Infiltration into Unsaturated–Semi-Saturated Soils

Transient fluid flow through unsaturated–saturated soil is generally described by Richards' equation.

This equation is obtained by the combination of continuity and Darcy's law as a momentum equation. This equation is expressed in different forms. The 2D θ -based form of the equation is (Richards 1931; Bear and Chang 2010):

$$\frac{\partial \theta}{\partial t} = \frac{\partial}{\partial x} \left(D_x(\theta) \frac{\partial \theta}{\partial x} \right) + \frac{\partial}{\partial z} \left(D_z(\theta) \frac{\partial \theta}{\partial z} + K_z(\theta) \right) \tag{1}$$

where $\theta \left(\frac{L^3}{L^3} \right)$ is the volumetric water content and $D(\theta) = K(\theta) \frac{\partial h}{\partial \theta}$ is soil water diffusivity for an isotropic media; $h(L)$ is the soil water pressure head (tension head in unsaturated zone), $K \left(\frac{L}{T} \right)$ is the hydraulic conductivity, $t(T)$ is the time and $Z(L)$ is the vertical space coordinate (upward positive). Water diffusivity, hydraulic conductivity and water content are functions of soil water pressure head. Various empirical relationships have been used to relate K and θ to h (Brooks and Corey 1964; Van Genuchten 1980; Haverkamp et al. 1990; Fredlund and Xing 1994). Basha (1999) described K and θ in terms of h by the exponential expression:

$$\frac{\theta - \theta_r}{\theta_s - \theta_r} = S = \exp(\alpha h) \tag{2}$$

$$K(\theta) = K_s \frac{\theta - \theta_r}{\theta_s - \theta_r} = K_s S = K_s \exp(\alpha h) \tag{3}$$

where θ_r is the residual water content, θ_s is the saturated water content, $K_s \left(\frac{L}{T} \right)$ is the saturated hydraulic conductivity and $\alpha \left(\frac{1}{L} \right)$ is the pore size distributions index. It is believed that the exponential model (Eqs. 2 and 3) for description of properties of unsaturated soils would pass physically reasonable criteria (Tracy 2006, 2007).

Substituting (2) and (3) in $D(\theta)$ gives:

$$D(\theta) = K(\theta) \frac{\partial h}{\partial \theta} = \frac{K_s}{\alpha(\theta_s - \theta_r)} \tag{4}$$

Substituting Eqs. (2), (3) and (4) in Eq. (1) provides a linear form of Richards' equation.

$$\frac{\partial \theta}{\partial t} = D \frac{\partial^2 \theta}{\partial x^2} + D \frac{\partial^2 \theta}{\partial z^2} + f \frac{\partial \theta}{\partial z} \tag{5}$$

where D and f are:

$$D = \frac{K_s}{\alpha(\theta_s - \theta_r)}, \quad f = \frac{K_s}{(\theta_s - \theta_r)} \tag{6}$$

Analytical solutions for Eq. (5) would express spatiotemporal distribution of water content in the unsaturated–saturated soil sample under given boundary and initial conditions.

3 Solution Domain for 2D Water Infiltration into Unsaturated–Semi-Saturated Soils

Richards' equation in a vertical 2D plane (x, z) may be expressed as Eq. (5):

$$\frac{\partial \theta}{\partial t} = D \frac{\partial^2 \theta}{\partial z^2} + f \frac{\partial \theta}{\partial z} + D \frac{\partial^2 \theta}{\partial x^2} \tag{7}$$

In order to obtain closed-form analytical solutions for this equation, many simplifications shall be employed. In the first step, vertical section of a homogeneous soil sample may be assumed, and then, the no-flow boundary condition is applied at the side edges and various distributions of water content are used at the top boundary. Also, different forms of the water table can be considered for initial condition in the 2D soil domain. In the current study, two forms of the water table are assumed for initial condition (Fig. 1), where high water content zone is considered as semi-saturated zone and residual water content zone is considered as unsaturated zone at initial time.

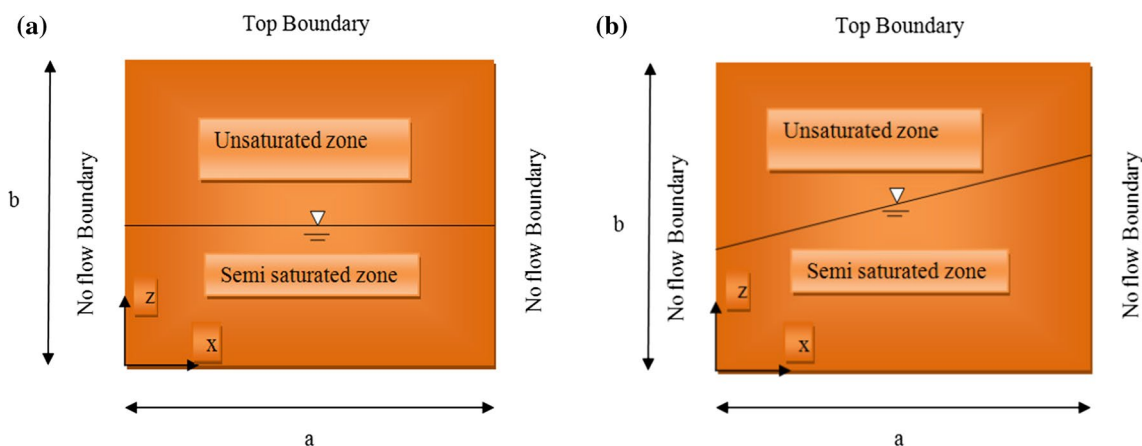


Fig. 1 The 2D soil domain for infiltration from top boundary a horizontal water table b steep water table

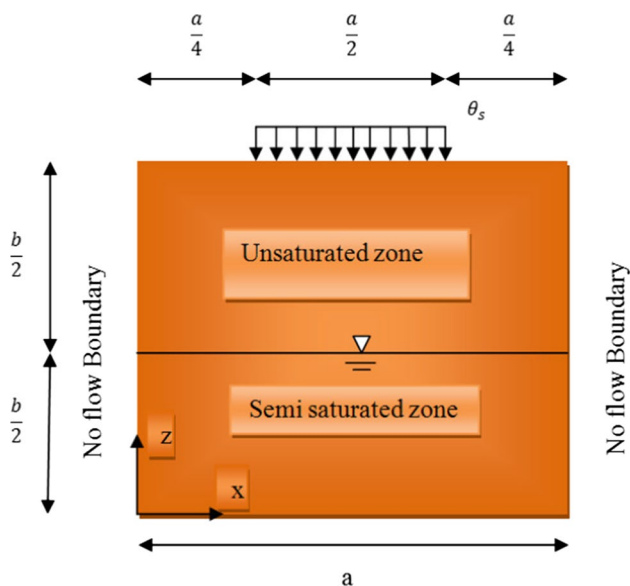


Fig. 2 Schematic view of 2D infiltration problem in case 1

4 Case 1: A Uniform Distribution of Water Content on a Part at the Top Boundary and a Horizontal Water Table Initial Condition

As a practical case, a uniform distribution of saturated water content is applied on a part at the top boundary and a horizontal water table is used for initial condition, where high water content zone is considered as semi-saturated zone and residual water content zone is considered as unsaturated zone at initial time. Also, no-flow boundary conditions are applied at right and left boundaries. A schematic view of the problem statement is shown in Fig. 2.

In this case, boundary and initial conditions may be mathematically expressed as:

$$\frac{\partial \theta}{\partial x}(0, z, t) = 0 \quad \frac{\partial \theta}{\partial x}(a, z, t) = 0 \quad (8-a)$$

$$\theta(x, b, t) = (\theta_s - \theta_r) * \left[U\left(x - \frac{a}{4}\right) - U\left(x - \frac{3a}{4}\right) \right] + \theta_r \quad (8-b)$$

$$\theta(x, 0, t) = \theta_0 \quad (8-c)$$

$$\theta(x, z, 0) = (\theta_r - \theta_0) * U\left[z - \frac{b}{2}\right] + \theta_0 \quad (8-d)$$

where θ_0 is high water content (very close to θ_s) and U is the unit step function. The boundary condition (8-b) at the top boundary creates saturated water content for all points of $\frac{a}{4} \leq x < \frac{3a}{4}$ and residual water content for all points of $0 \leq x < \frac{a}{4}$ and $\frac{3a}{4} \leq x < a$. Also, the initial condition (8-d)

creates high water content for all points of $0 \leq z < \frac{b}{2}$ and residual water content for all points of $\frac{b}{2} \leq z < b$.

Analytically, setting up and developing these boundary and initial conditions for the cases are the main innovations of this research. Based on existing researches, these types of analytical boundary and initial conditions have not been presented for unsaturated–semi-saturated soils.

A single closed-form analytical solution is sought that encompasses both steady and unsteady solutions. Thus, the general form of such a solution may be expressed as a combination of a steady (W) and an unsteady (V) term:

$$\theta(x, z, t) = \varphi(x, z, t) + \psi(x, z) \quad (9)$$

Obviously, non-homogenous boundary conditions are to satisfy $\psi(x, z)$, the steady solution, and homogenous boundary conditions are for $\varphi(x, z, t)$, the unsteady solution. Substituting (9) in (7) and (8-a) to (8-d) and then utilizing separation of variables for $\psi(x, z)$ and $\varphi(x, z, t)$ yield:

$$\begin{aligned} \theta(x, z, t) = & \sum_{m=1}^{\infty} \sum_{n=1}^{\infty} D_{mn} \cos\left(\frac{n\pi x}{a}\right) \\ & \sin\left(\frac{m\pi z}{b}\right) e^{-\frac{f}{2D}z} e^{-\left(\beta^2 + \nu^2 + \left(\frac{f}{D}\right)^2 \frac{1}{4}\right)Dt} \\ & + \sum_{m=1}^{\infty} D_m e^{-\frac{f}{2D}z} \sin\left(\frac{m\pi z}{b}\right) e^{-\left(\eta^2 + \left(\frac{f}{D}\right)^2 \frac{1}{4}\right)Dt} \\ & + \sum_{n=1}^{\infty} e^{-\frac{f}{2D}z} \cos\left(\frac{n\pi x}{a}\right) \\ & [C_1^{**} \sinh(\tau z) + C_2^{**} \cosh(\tau z)] + C_3^{**} z + C_4^{**} e^{-\frac{f}{D}z} \end{aligned} \quad (10)$$

where $\beta = \frac{n\pi}{a}$, $\nu = \eta = \frac{m\pi}{b}$, $\tau = \sqrt{\frac{1}{4}\left(\frac{f}{D}\right)^2 + \beta^2}$ and D_{mn} , D_m , C_1^{**} , C_2^{**} , C_3^{**} and C_4^{**} are constant coefficients. The constant coefficients are expressed as:

$$C_1^{**} = \frac{2e^{\frac{f}{2D}b}}{n\pi \sinh(\tau b)} * \left((\theta_r - \theta_s) \sin\left(\frac{n\pi}{4}\right) - (\theta_s - \theta_r) \sin\left(\frac{3n\pi}{4}\right) \right) \quad (11-a)$$

$$C_2^{**} = 0 \quad (11-b)$$

$$C_3^{**} = \frac{\frac{1}{2}(\theta_s + \theta_r) - \theta_s e^{-\frac{f}{D}b}}{b} \quad (11-c)$$

$$C_4^{**} = \theta_0 \quad (11-d)$$

$$\begin{aligned} D_{mn} = & \frac{-C_1^{**}(-1)^{m+1} a^2 m \pi \left(e^{\frac{2\sqrt{ha^2+n^2\pi^2}b}{a}} - 1 \right) e^{-\frac{\sqrt{ha^2+n^2\pi^2}b}{a}}}{b^2 \pi^2 n^2 + a^2 b^2 h + m^2 \pi^2 a^2}, \\ h = & \frac{1}{4} \left(\frac{f}{D} \right)^2 \end{aligned} \quad (11-e)$$

$$\begin{aligned}
 D_m &= A_1(A_2 + A_3 \sin\left(\frac{m\pi}{2}\right) + A_4 \cos\left(\frac{m\pi}{2}\right) + A_5 + A_6 - A_7 \\
 A_1 &= \frac{2}{f^2b^2 + 4m^2\pi^2D^2}, A_2 = 4D^2m\theta_r\pi(-1)^{m+1}e^{\frac{fb}{2D}}, A_3 = 2Dbf e^{\frac{fb}{4D}}(\theta_0 - \theta_r) \\
 A_4 &= 4D^2m\pi e^{\frac{fb}{4D}}(\theta_r - \theta_0), A_5 = \frac{8m\pi D^2\theta_0}{f^2b^2 + 4m^2\pi^2D^2} \\
 A_6 &= \frac{8C_3^{**}m\pi D^2b\left(4Dbf + 4e^{\frac{fb}{2D}}(-1)^m m^2\pi^2D^2 + e^{\frac{fb}{2D}}(-1)^m f^2b^2 + 4e^{\frac{fb}{2D}}(-1)^{m+1}Dbf\right)}{f^4b^4 + 8f^2b^2m^2\pi^2D^2 + 16m^4\pi^4D^4} \\
 A_7 &= \frac{8m\pi D^2\theta_s C_4^{**}\left(e^{\frac{fb}{2D}} - (-1)^m\right)e^{-\frac{fb}{2D}}}{f^2b^2 + 4m^2\pi^2D^2}
 \end{aligned}
 \tag{11-f}$$

Further details for derivation of Eq. (10) are presented in “Appendix”. As seen, Eq. (10) consists of five terms: a function of (x, z, t) , a function of (z, t) , a function of (x, z) and two functions of z only. All boundary and initial conditions of (8-a) to (8-d), as well as the PDE (Eq. 7), are satisfied by (10). The first two terms in Eq. (10) demonstrate unsteady behavior of the infiltrating water content front. However, the last three terms are not functions of time and reflect the steady behavior of the front. Obviously, as $t \rightarrow \infty$, the first two terms vanish and the solution approaches to steady-state solution. In Eq. (10), summation convergence occurs very rapidly, partly because n and m (showing number of terms in the summation) lie in denominators of summations coefficients. Furthermore, due to the presence of a time-dependent exponential decay term in the first term of Eq. (10), many terms are needed for summation calculation at early times, while at longer times, often a handful of terms is sufficient to obtain a reasonable accuracy. In order to confirm summations convergence in Eq. (10), water content at different positions is calculated using summations truncation with different values of n and m (Table 1). The table is generated for the following parameters:

$$\begin{aligned}
 t &= 20 \text{ min}, \quad a = 100 \text{ cm}, \quad b = 100 \text{ cm}, \\
 \theta_0 &= 0.3, \quad \theta_r = 0.0286, \quad \theta_s = 0.3658, \\
 \alpha &= 0.01 \frac{1}{\text{cm}}, \quad K_s = 10^{-3} \frac{\text{cm}}{\text{s}}
 \end{aligned}$$

To be consistent with the literature, $\theta_0, \theta_r, \theta_s, \alpha$ and K_s values studied by Huang and Wu (2012); and Montazeri Namin and Boroomand (2012) are selected. As given in Table 1, change in water content is negligible at n and $m = 1 \sim 15$ and higher. As a consequence, θ was calculated for $n = m = 1 \sim 15$ in Eq. (10). In order to indicate the use of the derived equations, water content values of an explicit scheme finite difference method (FDM) solution (to Eq. 7) are compared to those of the analytical solution (Eq. 10) for $t = 20$ min and various values of x and z (column 7 in Table 1). More details for the explicit FDM solution can be found in Bear and Chang (2010).

Eighth column in Table 1 shows relative error (RE) based on column 5 (incorporating > 250 summation terms) and column 7 (FDM for $\Delta t = 5$ s, $\Delta z = 5$ cm and $\Delta x = 5$ cm). Relative error (RE) is expressed as:

Table 1 Water content values for the analytical solution (with different summation truncations), FDM solution and the relative error for case 1 at $t = 20$ min

x (cm)	z (cm)	$\theta_{\text{Analytical}}, m=n=1 \sim 5$	$\theta_{\text{Analytical}}, m=n=1 \sim 10$	$\theta_{\text{Analytical}}, m=n=1 \sim 15$	$\theta_{\text{Analytical}}, m=n=1 \sim 20$	$\theta_{\text{FDM}}, \Delta t=5 \text{ s}, \Delta z=\Delta x=5 \text{ cm}$	RE (%)
25	30	0.2435	0.2558	0.2572	0.2572	0.2604	1.24
40	50	0.1998	0.2001	0.2009	0.2009	0.2036	1.34
50	80	0.1978	0.1982	0.1992	0.1992	0.2021	1.45
60	90	0.2562	0.2568	0.2577	0.2577	0.2532	1.74
50	95	0.3103	0.3110	0.3119	0.3119	0.3164	1.44
70	40	0.2288	0.2292	0.2301	0.2301	0.2337	1.56
80	20	0.2758	0.2762	0.2773	0.2773	0.2726	1.69
90	85	0.1005	0.1008	0.1020	0.1020	0.1031	1.07
10	60	0.1601	0.1606	0.1617	0.1617	0.1634	1.05
30	70	0.1582	0.1589	0.1593	0.1593	0.1612	1.19

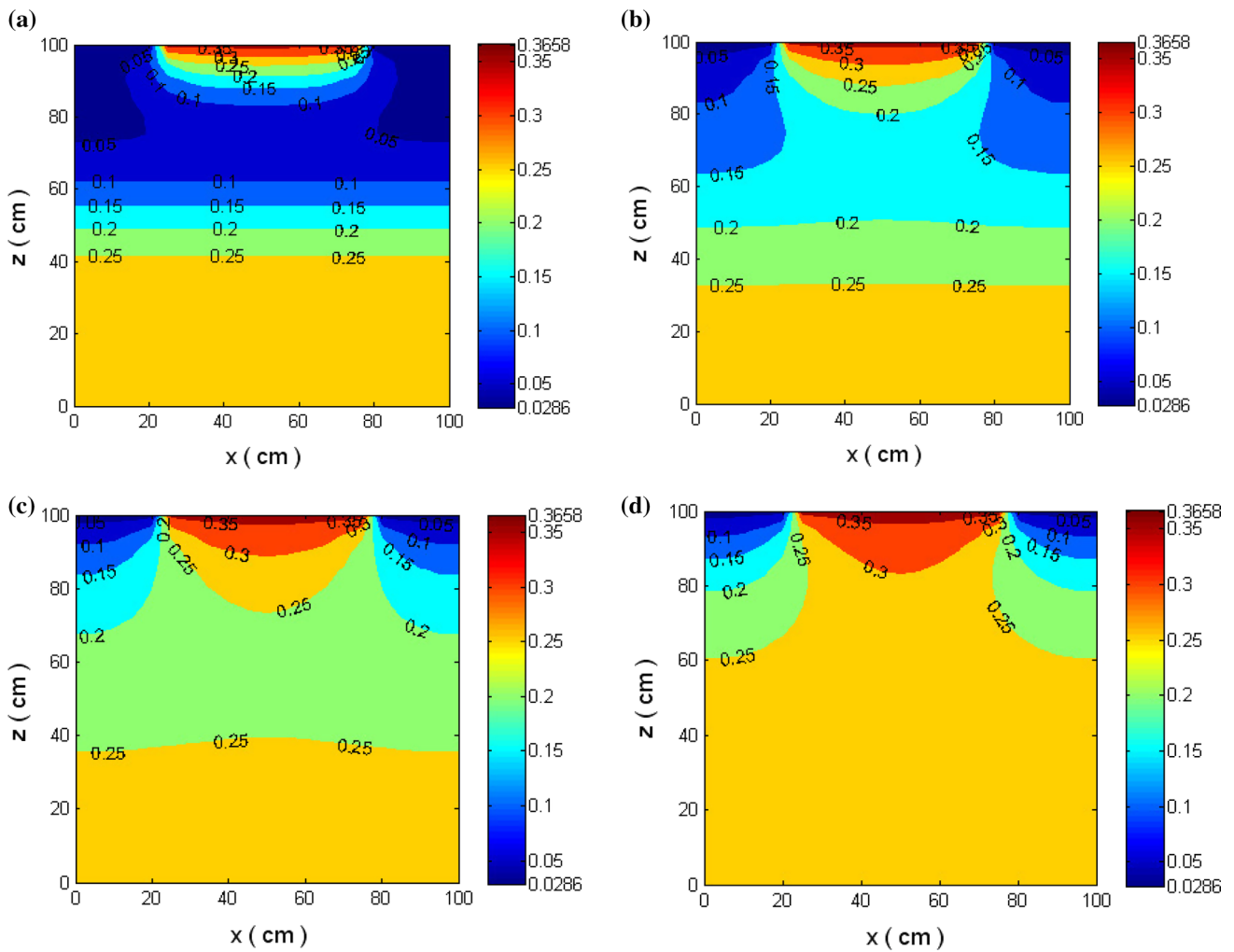


Fig. 3 Water content contours based on Eq. (10) for: a $t=5$ min, b $t=20$ min, c $t=60$ min and d steady state

$$\text{Relative Error} = \frac{|\theta_{\text{Analytical}} - \theta_{\text{Numerical}}|}{|\theta_{\text{Analytical}}|} \times 100\% \quad (12)$$

As given in Table 1, errors are all less than 2% which may be deemed reasonable. It should be considered that it is possible to find a numerical method or software which leads to higher degree of accuracy. However, this developed analytical solution is benchmark solution for verification and efficiency assessment of numerical methods.

Based on Eq. (10), water content contours are shown in Fig. 3a–d for $t=5, 20, 60$ min and steady state, respectively. As shown in the figures, the infiltrating water content front begins from a part at the top boundary ($\frac{a}{4} \leq x < \frac{3a}{4}$)

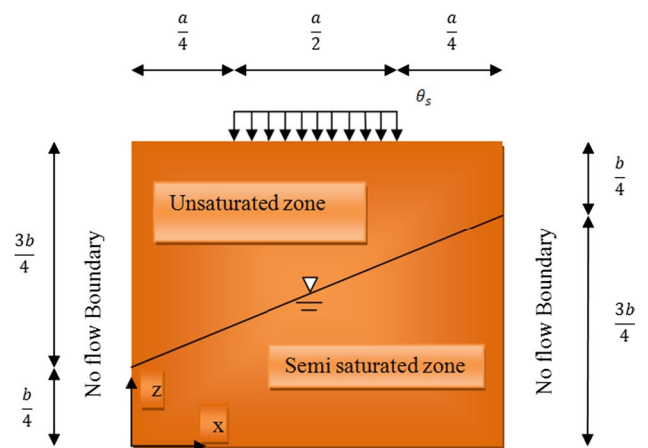


Fig. 4 Schematic view of 2D infiltration problem in case 2

and covers the entire unsaturated zone by time. The vertical advancement of the water content front into the drier parts of the sample is symmetric relative to $x = a/2$. Obviously, as $t \rightarrow \infty$, the water content values increase at all regions and the water table moves toward the soil sample surface as it converts from horizontal to curve form. Evidently, water content contours are perpendicular to the right and left boundaries of the soil sample, confirming no-flow boundary condition in those boundaries. Also, as time elapses, water content contours approach a steady-state contour associated with the last three terms in Eq. (10) (Fig. 3d).

5 Case 2: A Uniform Distribution of Water Content on a Part at the Top Boundary and an Inclined Water Table Initial Condition

There is naturally an inclined water table due to gradient differences in many aquifers (Deng and Wang 2017; Ruhaak et al. 2008; Ameli et al. 2013; Saeedpanah and Golmohamadi Azar 2017; Schnellmann et al. 2010). Herein, a practical case is considered whereby ground surface ponding occurs on a part of the top boundary for the unsaturated–semi-saturated aquifer with inclined water table at initial time. Also, the right and left boundaries are considered as no-flow

boundaries. A schematic view of the problem statement is shown in Fig. 4.

Boundary and initial conditions for this case may be written mathematically as:

$$\frac{\partial \theta}{\partial x}(0, z, t) = 0 \quad \frac{\partial \theta}{\partial x}(a, z, t) = 0 \tag{13-a}$$

$$\theta(x, b, t) = (\theta_s - \theta_r) * \left[U\left(x - \frac{a}{4}\right) - U\left(x - \frac{3a}{4}\right) \right] + \theta_r \tag{13-b}$$

$$\theta(x, 0, t) = \theta_0 \tag{13-c}$$

$$\theta(x, z, 0) = (\theta_r - \theta_0) * U\left[z - \left(\frac{b}{2a}x + \frac{b}{4}\right)\right] + \theta_0 \tag{13-d}$$

The initial condition of (13-d) creates high water content for all points of the semi-saturated zone and residual water content for all points of the unsaturated zone in Fig. 4. Another innovation of this research is creation and expression of the initial condition analytically for the problem. Based on existing researches, this type of analytical initial condition has not been presented for the unsaturated–semi-saturated soils.

Following similar mathematical procedures as before (case 1 and “Appendix”), the answer for $\theta(x, z, t)$ would be identical to Eq. (10) but with different coefficients. The mathematical forms of C_1^{**} , C_2^{**} , C_3^{**} and C_4^{**} are identical to what were defined by Eqs. (11-a) to (11-d). However, coefficients of D_{mn} and D_m are expressed as:

$$D_{mn} = \frac{4}{ab} \int_0^b \int_0^a \{(\theta_r - \theta_0) * U\left[z - \left(\frac{b}{2a}x + \frac{b}{4}\right)\right] + \theta_0 - \psi(x, z)\} e^{\frac{t}{2b}z} \sin\left(\frac{m\pi}{b}z\right) \cos\left(\frac{n\pi}{a}x\right) dx dz =$$

$$D_{mn} = \frac{(\sin\left(\frac{3m\pi}{4}\right) \sin\left(\frac{n\pi b}{2a}\right) C_1 + \sin\left(\frac{m\pi}{4}\right) C_2 + \sin\left(\frac{3m\pi}{4}\right) \cos\left(\frac{n\pi b}{2a}\right) C_3 + \cos\left(\frac{3m\pi}{4}\right) \sin\left(\frac{n\pi b}{2a}\right) C_4 + \sin\left(\frac{n\pi b}{2a}\right) C_5 + (\cos\left(\frac{m\pi}{4}\right) - \cos\left(\frac{3m\pi}{4}\right) \cos\left(\frac{n\pi b}{2a}\right)) C_6}{C_7} + C_8 \tag{14-a}$$

$$C_1 = 8a^4 b^3 D e^{\frac{3b}{2b}} (\theta_0 - \theta_r) f^3 + 32a^2 b D^3 e^{\frac{3b}{2b}} f \pi^2 (a^2 \theta_0 m^2 - b^2 \theta_r n^2 - a^2 \theta_r m^2)$$

$$C_2 = 16D^2 e^{\frac{b}{2b}} (\theta_0 - \theta_r) (4ab^3 f^3 n^3 \pi^3 D^2 + a^3 b^3 f^2 n \pi - 4a^3 b f^3 n m^2 \pi^3 D^2)$$

$$C_3 = 16D^2 e^{\frac{3b}{2b}} (\theta_0 - \theta_r) (4ab^3 f^3 n^3 \pi^3 D^2 - 4a^3 b D^2 n m^2 \pi^3 + a^3 b^3 f^2 n \pi)$$

$$C_4 = 16D^2 e^{\frac{3b}{2b}} (4a^4 (\theta_r - \theta_0) (m^3 \pi^3 D^2 + b^2 m \pi f^2) - 4a^2 D^2 b^2 \pi^3 n^2 \theta_r m)$$

$$C_5 = 32a^2 D^3 b^3 e^{\frac{3b}{2b}} n^2 \pi^2 \theta_0 (\sin\left(\frac{3m\pi}{4}\right) + 2 \cos\left(\frac{3m\pi}{4}\right))$$

$$C_6 = 64a^3 D^3 b^2 e^{\frac{3b}{2b}} f \pi^2 (\theta_r - \theta_0) m n$$

$$C_7 = n \pi f^4 a^4 b^4 + 8n \pi^3 f^2 a^2 b^2 D^2 (a^2 m^2 + b^2 n^2) + 16 \pi^5 D^4 (n m^4 a^4 + n^5 b^4) - 32 n^3 \pi^5 D^4 m^2 a^2 b^2$$

$$C_8 = \frac{-C_1^{**} (-1)^{m+1} a^2 m \pi (e^{\frac{2\sqrt{h a^2 + n^2 x^2}}{a}} - 1) e^{-\frac{\sqrt{h a^2 + n^2 x^2}}{a}}}{b^2 \pi^2 n^2 + a^2 b^2 h + m^2 \pi^2 a^2}$$

Table 2 Water content values for the analytical solution (with different summation truncations), FDM solution and the relative error for case 2 at $t=20$ min

x (cm)	z (cm)	$\theta_{\text{Analytical}}, m=n=1 \sim 5$	$\theta_{\text{Analytical}}, m=n=1 \sim 10$	$\theta_{\text{Analytical}}, m=n=1 \sim 15$	$\theta_{\text{Analytical}}, m=n=1 \sim 20$	$\theta_{\text{FDM}}, \Delta t=5$ s, $\Delta z=\Delta x=5$ cm	Relative error (%)
25	30	0.2199	0.2212	0.2218	0.2218	0.2245	1.21
40	50	0.1752	0.1779	0.1783	0.1783	0.1814	1.73
50	80	0.1998	0.2003	0.2008	0.2009	0.1983	1.29
60	90	0.2621	0.2631	0.2645	0.2647	0.2694	1.77
50	95	0.3106	0.3111	0.3125	0.3128	0.3174	1.47
70	40	0.2452	0.2457	0.2461	0.2461	0.2503	1.70
80	20	0.2853	0.2859	0.2861	0.2862	0.2812	1.74
90	85	0.1281	0.1285	0.1291	0.1294	0.1311	1.31
10	60	0.1120	0.1123	0.1124	0.1124	0.1140	1.42
30	70	0.1341	0.1346	0.1348	0.1348	0.1366	1.33

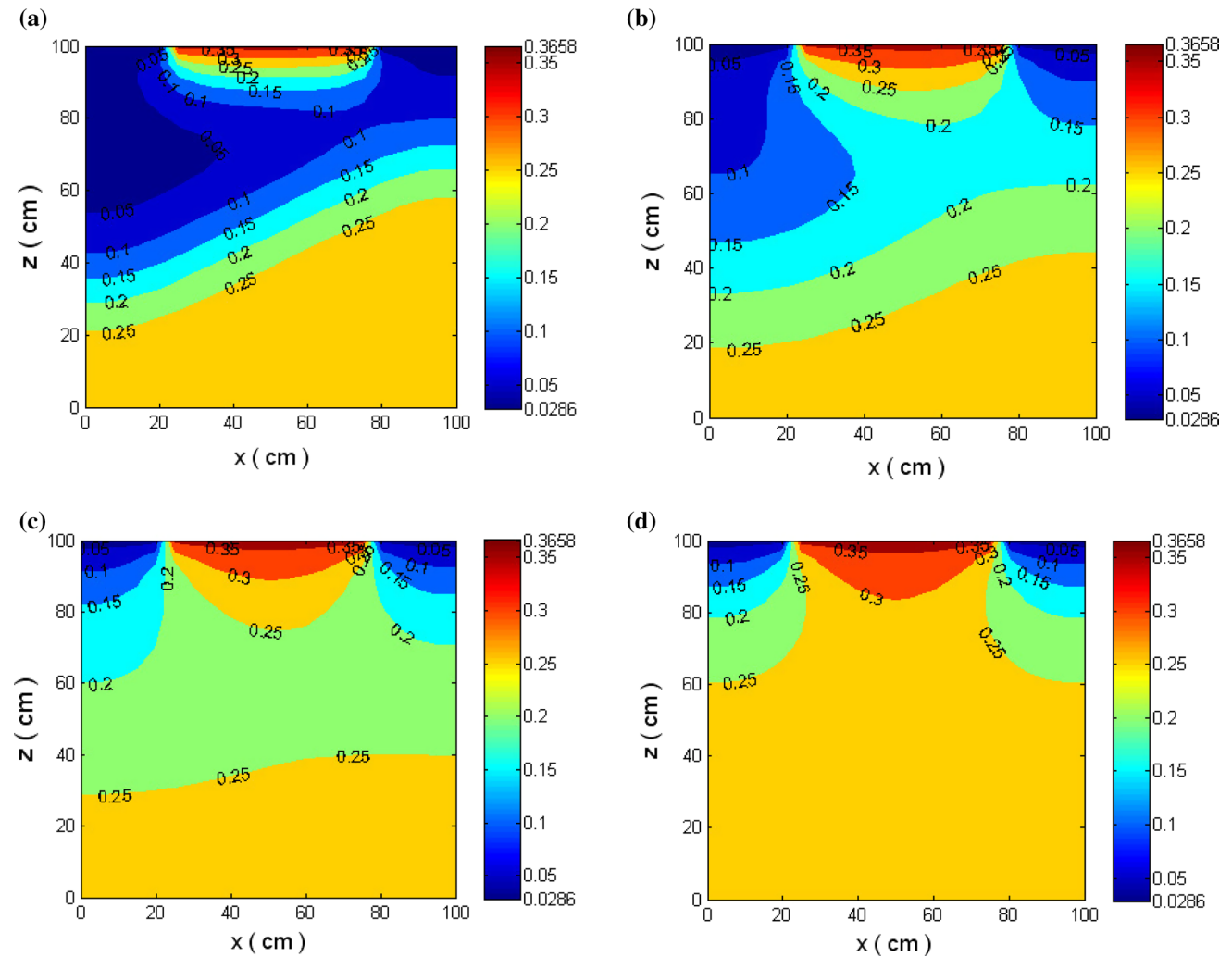


Fig. 5 Water content contours for case 2 at: **a** $t=5$ min, **b** $t=20$ min, **c** $t=60$ min and **d** steady state

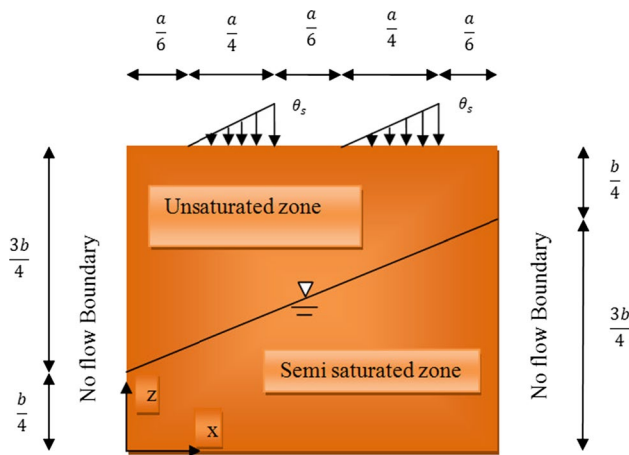


Fig. 6 Schematic view of 2D infiltration problem in case 3

in Eq. (10). To verify the developed solution, water content values obtained by an explicit scheme finite difference method (FDM) solution (to Eq. 7) is compared to those of the analytical solution (Eq. 10) for $t = 20$ min (column 7 in Table 2). Eighth column shows relative error (Eq. 12) calculated based on column 5 (incorporating > 250 summation terms) and column 7 (FDM for $\Delta t = 5$ s, $\Delta z = 5$ cm and $\Delta x = 5$ cm). As indicated, errors are all less than 2% which may be considered reasonable.

Based on Eqs. (10), (14-a) and (14-b), water content contours are shown in Fig. 5a–d for $t = 5, 20, 60$ min and steady state, respectively. As shown in the figures, the infiltrating water content front begins from a part at the top boundary ($\frac{a}{4} \leq x < \frac{3a}{4}$) and covers the entire unsaturated zone by time. Obviously, as $t \rightarrow \infty$, the water content values increase at all regions and the water table moves toward the soil sample surface as it converts from inclined shape to horizontal and

$$D_m = \frac{2}{ab} \int_0^b \int_0^a \{(\theta_r - \theta_0) * U[z - (\frac{b}{2a}x + \frac{b}{4})] + \theta_0 - \psi(x, z)\} e^{\frac{f}{2D}z} \sin(\frac{m\pi}{b}z) dx dz$$

$$D_m = C_{13}(\sin(\frac{3m\pi}{4})C_9 + \sin(\frac{m\pi}{4})C_{10} + \cos(\frac{3m\pi}{4})C_{11} + \cos(\frac{m\pi}{4})C_{12}) + C_{14} + C_{15} - C_{16} - C_{17}$$

$$C_9 = e^{\frac{3fb}{8D}}(\theta_0 - \theta_r)(4D^3b^2fm^2\pi^2(b + 2a) + 4D^2b^4f^2 + Db^5f^3 + 16D^4b^2m^2\pi^2 + 2Db^4af^3)$$

$$C_{10} = e^{\frac{fb}{8D}}(\theta_0 - \theta_r)(4D^2b^4f^2 - 16D^4b^2m^2\pi^2)$$

$$C_{11} = e^{\frac{3fb}{8D}}(\theta_r - \theta_0)(2D^2b^4m\pi f^2 - 16D^3b^3m\pi f + 16D^4abm^3\pi^3 + 4D^2b^3am\pi f^2 + 8D^4b^2m^3\pi^3)$$

$$C_{12} = 16D^3b^3m\pi f e^{\frac{fb}{8D}}(\theta_r - \theta_0)$$

$$C_{13} = \frac{2}{ab(f^4b^4 + 8f^2b^2m^2\pi^2D^2 + 16m^4\pi^4D^4)}$$

$$C_{14} = \frac{8m\pi D^2\theta_0}{f^2b^2 + 4m^2\pi^2D^2}$$

$$C_{15} = \frac{8C_3^{**}m\pi D^2b(4Dbf + 4e^{\frac{fb}{2D}}(-1)^m m^2\pi^2D^2 + e^{\frac{fb}{2D}}(-1)^m f^2b^2 + 4e^{\frac{fb}{2D}}(-1)^{m+1}Dbf)}{f^4b^4 + 8f^2b^2m^2\pi^2D^2 + 16m^4\pi^4D^4}$$

$$C_{16} = \frac{8m\pi D^2\theta_s C_4^{**}(e^{\frac{fb}{2D}} - (-1)^m)e^{-\frac{fb}{2D}}}{f^2b^2 + 4m^2\pi^2D^2}$$

$$C_{17} = 4D^2b\theta_r am\pi e^{\frac{fb}{2D}}(-1)^m(4D^2m^2\pi^2 + b^2f^2)$$
(14-b)

In order to confirm summations convergence in Eq. (10) with the new coefficients, water content at different positions is calculated using summations truncation with different n and m values (Table 2). The soil parameters used for the problem are identical to those used in case 1. As given in Table 2, change in water content is negligible at n and $m = 1 \sim 15$ and higher. As a consequence, θ is calculated for $n = m = 1 \sim 15$

curve shapes. Evidently, water content contours are perpendicular to the right and left boundaries of the soil sample, confirming no-flow boundary condition in those boundaries. Also, as time elapses, water content contours approach a steady-state contour (Fig. 5d) associated with the last three terms in Eq. (10) and the steady-state contour for this case approaches the steady-state contour for case 1 (Fig. 3d).

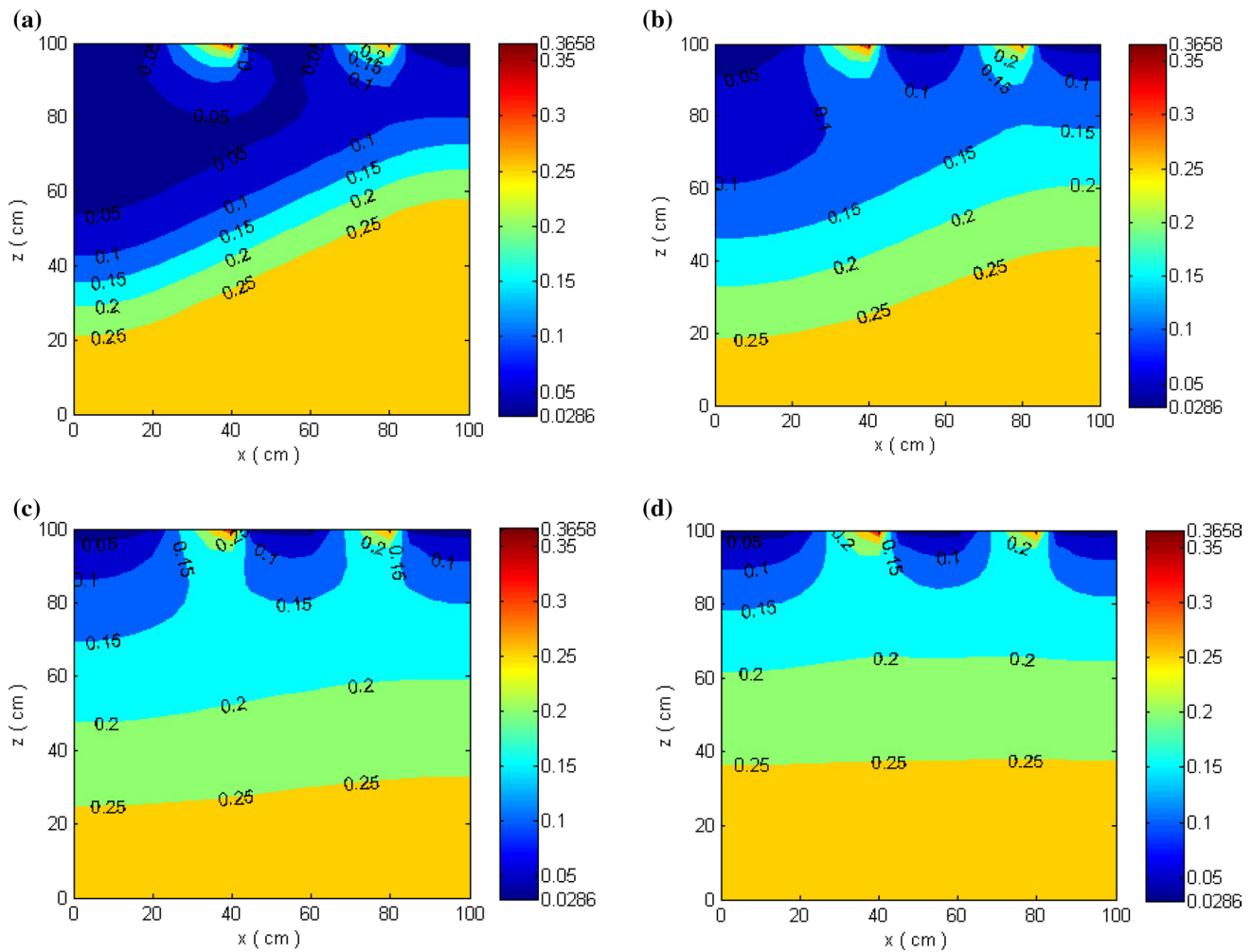


Fig. 7 Water content contours for case 3 at: **a** $t=5$ min, **b** $t=20$ min, **c** $t=60$ min and **d** steady state

6 Case 3: Ramp Distributions of Water Content on Two Parts at the Top Boundary and a Steep Water Table Initial Condition

In some cases, ground surface ponding in one part may also have a non-uniform distribution (Batu 1983; Wallach et al. 1991; Kim and Hong Kim 2018), which needs to be analyzed analytically. This case is similar to the previous case,

except for the fact that two parts of the top boundary are subjected to a ramp distribution of water content increasing linearly from θ_r to θ_s . A schematic view of the problem statement is shown in Fig. 6.

Boundary and initial conditions may be mathematically expressed as:

$$\frac{\partial \theta}{\partial x}(0, z, t) = 0 \quad \frac{\partial \theta}{\partial x}(a, z, t) = 0 \quad (15-a)$$

$$\theta(x, b, t) = (\theta_s - \theta_r)$$

$$\begin{aligned} & * \left[U\left(x - \frac{a}{6}\right)\left(\frac{4}{a}x - \frac{2}{3}\right) - U\left(x - \frac{5a}{12}\right)\left(\frac{4}{a}x - \frac{2}{3}\right) + U\left(x - \frac{7a}{12}\right)\left(\frac{4}{a}x - \frac{7}{3}\right) \right. \\ & \left. - U\left(x - \frac{5a}{6}\right)\left(\frac{4}{a}x - \frac{7}{3}\right) \right] + \theta_r \end{aligned} \quad (15-b)$$

$$\theta(x, 0, t) = \theta_0 \quad (15-c)$$

$$\theta(x, z, 0) = (\theta_r - \theta_0) * U\left[z - \left(\frac{b}{2a}x + \frac{b}{4}\right)\right] + \theta_0 \quad (15-d)$$

The boundary condition (15-b) at the top boundary creates linear distribution (ramp distribution) of water content from θ_r to θ_s for all points of $\frac{a}{6} \leq x < \frac{5a}{12}$ and $\frac{7a}{12} \leq x < \frac{5a}{6}$ (corresponding to Fig. 6). Creation and expression of the boundary condition analytically for the problem is another innovation of this research. This type of the analytical boundary condition has not been presented in previous studies for non-uniform distribution of ground surface ponding on the top boundary of the unsaturated–semi-saturated soils. Following similar mathematical procedures as before (case 1 and “Appendix”), the answer for $\theta(x, z, t)$ would be identical to Eq. (10) but with different coefficients. The mathematical forms of C_2^{**} , C_4^{**} , D_{mn} and D_m are identical to what were defined by Eqs. (11-a), (11-d), (14-a) and (14-b), respectively. The mathematical forms of C_1^{**} and C_3^{**} in this case are:

$$\begin{aligned} C_1^{**} &= \frac{2e^{\frac{f}{2D}b}}{a \sinh(\tau b)} \int_0^a ((\theta_s - \theta_r) \\ &* \left[U\left(x - \frac{a}{6}\right)\left(\frac{4}{a}x - \frac{2}{3}\right) - U\left(x - \frac{5a}{12}\right)\left(\frac{4}{a}x - \frac{2}{3}\right) + U\left(x - \frac{7a}{12}\right)\left(\frac{4}{a}x - \frac{7}{3}\right) \right. \\ &\left. - U\left(x - \frac{5a}{6}\right)\left(\frac{4}{a}x - \frac{7}{3}\right) \right] + \theta_r) \cos(\beta x) dx \\ &= \frac{2e^{\frac{f}{2D}b}}{n^2 \pi^2 \sinh(\tau b)} \\ &* \left(4(\theta_s - \theta_r) \cos\left(\frac{5n\pi}{12}\right) + 4(\theta_r - \theta_s) \cos\left(\frac{n\pi}{6}\right) + 4(\theta_r - \theta_s) \cos\left(\frac{7n\pi}{12}\right) \right. \\ &+ 4(\theta_s - \theta_r) \cos\left(\frac{5n\pi}{6}\right) \\ &\left. + n\pi(\theta_s - \theta_r) \sin\left(\frac{5n\pi}{6}\right) + n\pi(\theta_s - \theta_r) \sin\left(\frac{5n\pi}{12}\right) \right) \end{aligned} \quad (16-a)$$

$$\begin{aligned} C_3^{**} &= \frac{1}{ab} \int_0^a ((\theta_s - \theta_r) \\ &* \left[U\left(x - \frac{a}{6}\right)\left(\frac{4}{a}x - \frac{2}{3}\right) - U\left(x - \frac{5a}{12}\right)\left(\frac{4}{a}x - \frac{2}{3}\right) + U\left(x - \frac{7a}{12}\right)\left(\frac{4}{a}x - \frac{7}{3}\right) \right. \\ &\left. - U\left(x - \frac{5a}{6}\right)\left(\frac{4}{a}x - \frac{7}{3}\right) \right] + \theta_r) dx - C_4^{**} e^{-\frac{f}{D}b} \\ &= \frac{1}{b} \left(\frac{1}{4}\theta_s + \frac{3}{4}\theta_r - \theta_s e^{-\frac{fb}{D}} \right) \end{aligned} \quad (16-b)$$

Similar to previous cases, θ in this case is calculated for $n=m=1-15$. Based on Eqs. (10), (14-a), (14-b), (16-a) and (16-b), water content contours are shown in Fig. 7a–d for $t=5, 20, 60$ min and steady state, respectively. Soil parameters used for the problem are identical to those used before.

As shown in the figures, water content just below the top boundary corresponds to the top boundary condition of Eq. (15-b) shown in Fig. 7 very closely, with the maximum water content always remaining at $x=41.6$ and 83.2 cm (corresponding to $x = \frac{5a}{12}$ and $\frac{5a}{6}$). Vertical advancements of the water content front into the drier parts of the sample are clearly portrayed in the figures. However, water content at the top boundary (other than the “recharging window”) remains at $\theta_r=0.0286$ during the front advancement. Water content contours would be perpendicular to the side boundaries, confirming no-flow boundary conditions there. Also, as time elapses, water content contours approach a steady-state contour (Fig. 7d) associated with the last three terms in Eq. (10) and the water table moves toward the soil sample surface as it converts from inclined form to horizontal and curve forms.

7 Conclusions

In this paper, exponential models for water content and hydraulic conductivity were selected for nonlinear Richards’

equation to become linear and then separation of variables and Fourier series expansion techniques were used to derive analytical solutions to 2D water infiltration into unsaturated–semi-saturated soils with different distributions of water content on a part and/or parts of the top boundary. 2D water infiltrations were investigated in a rectangular soil domain, where high water content zone was considered as semi-saturated zone and residual water content zone was considered as unsaturated zone at initial time. A total of three cases were investigated in this paper. In case 1, a uniform distribution of water content on a part at the top boundary and no-flow boundaries at side edges were considered. Also, horizontal water table in unsaturated–semi-saturated domain was assumed as initial condition. In case 2, an inclined water table initial condition and a uniform distribution of water content on a part at the top boundary were investigated. Finally, in case 3, an analytical solution for ramp distributions of water content on two parts at the top boundary and an inclined water table initial condition was obtained.

Analytically, setting up and developing these boundary and initial conditions for the cases are the main innovations of this research. Based on existing researches, these types of analytical boundary and initial conditions have not been presented for unsaturated–semi-saturated soils.

All the boundary and initial conditions in each case, as well as governing equation, were satisfied by the presented analytical solutions. Vertical advancements of the water content front into the drier parts of the sample were clearly portrayed in the figures of each case. Analytical solutions for cases 1 and 2 were compared to numerical finite difference method solutions and shown to have less than 2% difference. It should be noted that it is possible to find a numerical method or software which leads to higher degree of accuracy. However, these developed analytical solutions are benchmark solution for verification and efficiency assessment of numerical methods. Also, these can be applied as the benchmark solutions which are vital for several analyses such as sensitivity analysis.

Appendix

Further details for derivation of Eq. (10) are as follows:

Substituting (9) in (7) and (8-a)–(8-d) yields:

$$D \frac{\partial^2 \varphi}{\partial z^2} + f \frac{\partial \varphi}{\partial z} + D \frac{\partial^2 \varphi}{\partial x^2} - \frac{\partial \varphi}{\partial t} = 0 \quad (17)$$

$$\frac{\partial \varphi}{\partial x}(0, z, t) = 0 \quad \frac{\partial \varphi}{\partial x}(a, z, t) = 0 \quad (18)$$

$$\varphi(x, 0, t) = 0 \quad \varphi(x, b, t) = 0 \quad (19)$$

$$\varphi(x, z, 0) = (\theta_r - \theta_0) * U\left[z - \frac{b}{2}\right] + \theta_0 - \psi(x, z) \quad (20)$$

Similarly, the PDE for $\psi(x, z)$ may be written as:

$$D \frac{\partial^2 \psi}{\partial z^2} + f \frac{\partial \psi}{\partial z} + D \frac{\partial^2 \psi}{\partial x^2} = 0 \quad (21)$$

$$\frac{\partial \psi}{\partial x}(0, z) = 0 \quad \frac{\partial \psi}{\partial x}(a, z) = 0 \quad (22)$$

$$\psi(x, b) = (\theta_s - \theta_r) * \left[U\left(x - \frac{a}{4}\right) - U\left(x - \frac{3a}{4}\right) \right] + \theta_r \quad (23)$$

$$\psi(x, 0) = \theta_0 \quad (24)$$

Now, utilizing separation of variables for $\psi(x, z)$:

$$\psi(x, z) = Z(z)X(x) \quad (25)$$

And substituting (25) in (21), one would get:

$$\frac{X''}{X} = -\left(\frac{Z''}{Z} + \frac{f}{D} \frac{Z'}{Z}\right) = \mu \quad (26)$$

where μ is an arbitrary constant. If $\mu = 0$ and $\mu < 0$, say $\mu = -\beta^2$ and $\beta > 0$, then with considering the boundary conditions of (22), $X(x)$ has two answers:

$$X = B^* \quad (27)$$

$$X_n = C_n^* \cos(\beta x), \quad \beta = \frac{n\pi}{a}, \quad n = 1, 2, 3, \dots, \infty \quad (28)$$

where B^* and C_n^* are constants. Substituting $\mu = 0$ and $\mu = -\beta^2$ in (26) for $\frac{X''}{X}$, two equations are obtained:

$$-\beta^2 = -\left(\frac{Z''}{Z} + \frac{f}{D} \frac{Z'}{Z}\right) \quad (29)$$

$$0 = -\left(\frac{Z''}{Z} + \frac{f}{D} \frac{Z'}{Z}\right) \quad (30)$$

The solutions of (29) and (30) are:

$$Z_n = e^{-\frac{f}{2D}z} [C_1^* \sinh(\tau z) + C_2^* \cosh(\tau z)] \quad (31)$$

$$Z_1 = C_3^* z + C_4^* e^{-\frac{f}{D}z} \quad (32)$$

where C_1^*, C_2^*, C_3^* and C_4^* are constants and $\tau = \sqrt{\frac{1}{4}\left(\frac{f}{D}\right)^2 + \beta^2}$. Substituting (27) and (32) in (25), an answer for $w(x, z)$ would be derived as:

$$\psi_1(x, z) = \left[C_3^{**} z + C_4^{**} e^{-\frac{f}{D}z} \right] \quad (33)$$

where C_3^{**} is $B^* C_3^*$ and C_4^{**} is $B^* C_4^*$. Substituting (28) and (31) in (25), another answer would be obtained for $w(x, z)$:

$$\psi_2(x, z) = \sum_{n=1}^{\infty} e^{-\frac{f}{2D}z} \cos\left(\frac{n\pi}{a}x\right) [C_1^{**} \sinh(\tau z) + C_2^{**} \cosh(\tau z)] \tag{34}$$

where C_1^{**} is $C_n^* C_1^*$ and C_2^{**} is $C_n^* C_2^*$. Now, $\psi(x, z)$ may be written as a combination of (33) and (34):

$$\begin{aligned} \psi(x, z) &= \psi_1(x, z) + \psi_2(x, z) \\ &= C_3^{**} z + C_4^{**} e^{-\frac{f}{D}z} + \sum_{n=1}^{\infty} e^{-\frac{f}{2D}z} \\ &\quad \cos\left(\frac{n\pi}{a}x\right) [C_1^{**} \sinh(\tau z) + C_2^{**} \cosh(\tau z)] \end{aligned} \tag{35}$$

Now, using (23), (24) and Fourier series properties, the constant coefficients in (35) would be:

$$C_2^{**} = \frac{2}{a} \int_0^a \theta_0 \cos(\beta x) dx \tag{36}$$

$$\begin{aligned} C_4^{**} &= \frac{1}{a} \int_0^a \theta_0 dx \\ C_1^{**} &= \frac{\frac{2}{a} e^{\frac{f}{2D}b} \int_0^a ((\theta_s - \theta_r) * [U(x - \frac{a}{4}) - U(x - \frac{3a}{4})]) + \theta_r \cos(\beta x) dx}{\sinh(\tau b)} \\ C_3^{**} &= \frac{\frac{1}{a} \int_0^a ((\theta_s - \theta_r) * [U(x - \frac{a}{4}) - U(x - \frac{3a}{4})]) + \theta_r dx - C_4^{**} e^{-\frac{f}{D}b}}{b} \end{aligned}$$

$\varphi(x, z, t)$ may be expressed via separation of variables as:

$$\varphi(x, z, t) = X(x)Z(z)T(t) \tag{37}$$

Substituting (37) in (17) and applying some simplifications gives:

$$\frac{X''}{X} = -\left(\frac{Z''}{Z} + \frac{f}{D} \frac{Z'}{Z} - \frac{1}{D} \frac{T'}{T}\right) = \mu \tag{38}$$

where μ is an arbitrary constant. If $\mu = 0$ and $\mu < 0$, say $\mu = -\beta^2$ and $\beta > 0$, then with considering the boundary conditions of (18), $X(x)$ has two answers:

$$X = A^* \tag{39}$$

$$X_n = D_n^* \cos(\beta x), \quad \beta = \frac{n\pi}{a}, \quad n = 1, 2, 3, \dots, \infty \tag{40}$$

where A^* and D_n^* are constants. Substituting $\mu = 0$ and $\mu = -\beta^2$ in (38) for $\frac{X''}{X}$, two equations are obtained:

$$-\beta^2 = -\left(\frac{Z''}{Z} + \frac{f}{D} \frac{Z'}{Z} - \frac{1}{D} \frac{T'}{T}\right) \tag{41}$$

$$0 = -\left(\frac{Z''}{Z} + \frac{f}{D} \frac{Z'}{Z} - \frac{1}{D} \frac{T'}{T}\right) \tag{42}$$

Substituting the boundary conditions of (19) in (41) gives:

$$Z_m = A_m^* e^{-\frac{f}{2D}z} \sin(vz), \quad v = \frac{m\pi}{b}, \quad m = 1, 2, 3, \dots, \infty \tag{43}$$

$$T(t) = A_{mn}^* e^{-\left(\beta^2 + v^2 + \left(\frac{f}{D}\right)^2 \frac{1}{4}\right)Dt} \tag{44}$$

where A_m^* and A_{mn}^* are constants. A similar procedure may be followed to obtain $Z(z)$ and $T(t)$ in (42):

$$Z_m = B_m^* e^{-\frac{f}{2D}z} \sin(\eta z), \quad \eta = \frac{m\pi}{b}, \quad m = 1, 2, 3, \dots, \infty \tag{45}$$

$$T = B_i^* e^{-\left(\eta^2 + \left(\frac{f}{D}\right)^2 \frac{1}{4}\right)Dt} \tag{46}$$

where B_m^* and B_i^* are constants. Substituting (40), (43) and (44) in (37), an answer for $\varphi(x, z, t)$ would be derived as:

$$\begin{aligned} \varphi_1(x, z, t) &= \sum_{m=1}^{\infty} \sum_{n=1}^{\infty} D_{mn} \cos\left(\frac{n\pi}{a}x\right) \\ &\quad \sin\left(\frac{m\pi}{b}z\right) e^{-\frac{f}{2D}z} e^{-\left(\beta^2 + v^2 + \left(\frac{f}{D}\right)^2 \frac{1}{4}\right)Dt} \end{aligned} \tag{47}$$

where D_{mn} is $D_n^* A_m^* A_{mn}^*$. Substituting (39), (45) and (46) in (37), another answer would be obtained for $\varphi(x, z, t)$:

$$\varphi_2(z, t) = \sum_{m=1}^{\infty} D_m e^{-\frac{f}{2D}z} \sin\left(\frac{m\pi}{b}z\right) e^{-\left(\eta^2 + \left(\frac{f}{D}\right)^2 \frac{1}{4}\right)Dt} \tag{48}$$

where D_m is $A^* B_m^* B_i^*$. Now, $\varphi(x, z, t)$ may be written as a combination of (47) and (48):

$$\begin{aligned} \varphi(x, z, t) &= \varphi_1(x, z, t) + \varphi_2(z, t) \\ &= \sum_{m=1}^{\infty} \sum_{n=1}^{\infty} D_{mn} \cos\left(\frac{n\pi}{a}x\right) \sin\left(\frac{m\pi}{b}z\right) e^{-\frac{f}{2D}z} e^{-\left(\beta^2 + v^2 + \left(\frac{f}{D}\right)^2 \frac{1}{4}\right)Dt} \\ &\quad + \sum_{m=1}^{\infty} D_m e^{-\frac{f}{2D}z} \sin\left(\frac{m\pi}{b}z\right) e^{-\left(\eta^2 + \left(\frac{f}{D}\right)^2 \frac{1}{4}\right)Dt} \end{aligned} \tag{49}$$

Substituting the initial condition of (20) in (49) and using Fourier series properties for (49), D_{mn} and D_m are written as:

$$D_{mn} = \frac{4}{ab} \int_0^b \int_0^a \{(\theta_r - \theta_0) * U\left[z - \frac{b}{2}\right] + \theta_0 - \psi(x, z)\} e^{\frac{f}{2D}z} \sin\left(\frac{m\pi}{b}z\right) \cos\left(\frac{n\pi}{a}x\right) dx dz \tag{50}$$

$$\begin{aligned} D_m &= \frac{2}{ab} \int_0^b \int_0^a \{(\theta_r - \theta_0) * U\left[z - \frac{b}{2}\right] \\ &\quad + \theta_0 - \psi(x, z)\} e^{\frac{f}{2D}z} \sin\left(\frac{m\pi}{b}z\right) dx dz \end{aligned}$$

Substituting (35) and (49) in (9), $\theta(x, z, t)$ or Eq. (10) is obtained.

References

- Ameli AA, Craig JR, Wong S (2013) Series solutions for saturated–unsaturated flow in multi-layer unconfined aquifers. *Adv Water Resour* 60:24–33
- Aquino J, Francisco AS, Pereira F, Amaral Souto HP, Furtado F (2007) Numerical simulation of transient water infiltration in heterogeneous soils combining central schemes and mixed finite elements. *Commun Numer Methods Eng* 23(6):491–505
- Basha HA (1999) Multidimensional linearized non steady infiltration with prescribed boundary conditions at the soil surface. *Water Resour Res* 35(1):75–83
- Batu V (1983) Flow net for two-dimensional linearized infiltration and evaporation from nonuniform and nonperiodic strip sources. *J Hydrol* 64:225–238
- Bear J, Chang AH (2010) Modeling groundwater flow and contaminant transport. Springer, Berlin
- Brooks RH, Corey AT (1964) Hydraulic properties of porous media. Colorado State University, Fort Collins **Hydrology Paper No. 3**
- Carr EJ, Turner IW (2014) Two-scale computational modelling of water flow in unsaturated soils containing irregular-shaped inclusions. *Int J Numer Methods Eng* 98(3):157–173
- Chen JM, Tan YC (2005) Analytical solutions of infiltration process under ponding irrigation. *Hydrol Process* 19(18):3593–3602
- Craig JR, Liu G, Soulis ED (2010) Runoff–infiltration partitioning using an upscaled Green–Ampt solution. *Hydrol Process* 24(16):2328–2334
- Cui G, Zhu J (2018) Prediction of unsaturated flow and water backfill during infiltration in layered soils. *J Hydrol* 557:509–521
- Deng B, Wang J (2017) Saturated–unsaturated groundwater modeling using 3D Richards equation with a coordinate transform of non-orthogonal grids. *Appl Math Model* 50:39–52
- Fredlund DG, Xing A (1994) Equations for soil-water characteristic curve. *Can Geotech J* 31(4):521–532
- Haverkamp R, Parlange JY, Starr JL, Schmitz GH, Fuentes C (1990) Infiltration under ponded conditions: 3. A predictive equation based on physical parameters. *Soil Sci J* 149(5):292–300
- Huang RQ, Wu LZ (2012) Analytical solutions to 1-D horizontal and vertical water infiltration in saturated/unsaturated soils considering time-varying rainfall. *Comput Geotech* 39:66–72
- Johari A, Hooshmand N (2015) Prediction of soil-water characteristic curve using gene expression programming. *Iran J Sci Technol Trans Civ Eng* 39(C1):143–165
- Kim C, Hong Kim D (2018) Effect of rainfall spatial distribution and duration on minimum spatial resolution of rainfall data for accurate surface runoff prediction. *J Hydro-environ Res* 20:1–8
- Li J, Wei C (2018) Explicit approximate analytical solutions of seepage-deformation in unsaturated soils. *Int J Numer Anal Methods Geomech* 42(7):943–956
- Montazeri Namin M, Boroomand MR (2012) A time splitting algorithm for numerical solution of Richard's equation. *J Hydrol* 444–445:10–21
- Mousavi Nezhad M, Javadi AA, Abbasi F (2011) Stochastic finite element modelling of water flow in variably saturated heterogeneous soils. *Int J Numer Anal Methods Geomech* 35(12):1389–1408
- Nasseri M, Shaghaghian MR, Daneshbod Y, Seyyedian H (2008) An analytic solution of water transport in unsaturated porous media. *J Porous Media* 11(6):591–601
- Richards LA (1931) Capillary conduction of liquids through porous mediums. *Physics* 1:318–333
- Ruhaak W, Rath V, Wolf A, Clauser C (2008) 3D finite volume groundwater and heat transport modeling with non-orthogonal grids, using a coordinate transformation method. *Adv Water Resour* 31:513–524
- Saeedpanah I, Golmohamadi Azar R (2017) New analytical solutions for unsteady flow in a leaky aquifer between two parallel streams. *Water Resour Manag* 31:2315–2332
- Schnellmann R, Busslinger M, Schneider HR, Rahardjo H (2010) Effect of rising water table in an unsaturated slope. *Eng Geol* 114:71–83
- Simunek J (2006) Models of water flow and solute transport in the unsaturated zone. *Encyclopedia of hydrological sciences*. Wiley Online Library, New York
- Su L, Wang J, Qin X, Wang Q (2017) Approximate solution of a one-dimensional soil water infiltration equation based on the Brooks–Corey model. *Geoderma* 297:28–37
- Tong JX, Yang JZ, Hu BX, Bao R (2010) Experimental study and mathematical modelling of soluble chemical transfer from unsaturated/saturated soil to surface runoff. *Hydrol Process* 24(21):3065–3073
- Tracy FT (2006) Clean two- and three-dimensional analytical solutions of Richards' equation for testing numerical solvers. *Water Resour Res* 42(8):W08503
- Tracy FT (2007) Three-dimensional analytical solutions of Richards' equation for a box-shaped soil sample with piecewise-constant head boundary conditions on the top. *J Hydrol* 336:391–400
- Van Genuchten MT (1980) A closed-form equation for predicting the hydraulic conductivity of unsaturated soils. *Soil Sci Soc Am J* 44(5):892–898
- Wallach R, Israeli M, Zaslavsky D (1991) Small-perturbation solution for steady nonuniform infiltration into soil surface of a general shape. *Water Resour Res* 27(7):1665–1670
- Wang K, Yang X, Liu X, Liu C (2017) A simple analytical infiltration model for short-duration rainfall. *J Hydrol* 555:141–154
- Wazwaz AM (2007) A comparison between the variational iteration method and Adomian decomposition method. *J Comput Appl Math* 207(1):129–136
- Zamra CE, Dumbser M, Toro EF, Moraga NO (2012) A novel numerical method of high-order accuracy for flow in unsaturated porous media. *Int J Numer Methods Eng* 89(2):227–240
- Zarif Sanayei HR, Rakhshandehroo GR, Talebbeydokhti N (2016) New analytical solutions to 2-D water infiltration and imbibition into unsaturated soils for various boundary and initial conditions. *Iran J Sci Technol Trans Civ Eng* 40(3):219–239
- Zarif Sanayei HR, Rakhshandehroo GR, Talebbeydokhti N (2017) Innovative analytical solutions to 1, 2 and 3D water infiltration into unsaturated soils for initial-boundary value problems. *Sci Iran* 24(5):2346–2368
- Zhan TLT, Jia GW, Chen Y, Fredlund DG, Li H (2013) An analytical solution for rainfall infiltration into an unsaturated infinite slope and its application to slope stability analysis. *Int J Numer Anal Methods Geomech* 37(12):1737–1760
- Zhu Y, Zha Y, Tong J, Yang J (2011) Method of coupling 1-D unsaturated flow with 3-D saturated flow on large scale. *Water Sci Eng* 4:357–373
- Zhu Y, Shi L, Lin L, Yang J, Ye M (2012) A fully coupled numerical modeling for regional unsaturated–saturated water flow. *J Hydrol* 475:188–203
- Zlotnik VA, Wang T, Nieber JL, Simunek J (2007) Verification of numerical solutions of the Richards equation using a traveling wave solution. *Adv Water Resour* 30:1973–1980